Coral Reefs (2026) 45:1805–1820
https://doi.org/10.1007/s00338-026-02872-5

RESEARCH

# Past thermal history and heat stress shape patterns of coral-algal symbioses in massive *Porites*

**Lindsey Kraemer**[1] · **David Juszkiewicz**[2] · **Zoe T. Richards**[2,3] · **Kate M. Quigley**[1,4,5]

Received: 30 July 2025 / Accepted: 7 April 2026 / Published online: 20 April 2026


**Abstract** Massive corals, like some *Porites* species, are key reef-builders and provide critical habitat on coral reefs. *Porites* often exhibit high tolerance to stressors, like warming from climate change, although the drivers of these patterns are unclear. Using high-throughput sequencing, we examined whether associations with Symbiodiniaceae underpin this tolerance. Symbiodiniaceae diversity and community composition within two massive species (*Porites lutea* and *P. lobata*), whose identities were verified through morphometric examinations, were characterised across 200 km of Ningaloo Coast World Heritage reef, Australia. Contrary to previous studies showing low diversity of high-fidelity algal symbionts, we found variability within *Cladocopium*, which differed significantly across host species and temperature metrics. *P. lobata* communities exhibited greater dispersion than those of *P. lutea*, suggesting higher among-colony variability in symbiont assemblages. Differential abundance analyses revealed both taxon-level and within-taxon (ASV-level) host specificity, including contrasting enrichments of closely related C15 variants between hosts. Locations with broader temperature ranges and a greater number of accumulated heat stress events (measured as Degree Heating Weeks ≥ 8 °C-weeks) exhibited significantly higher prevalence and abundance of thermotolerant *Cladocopium* C116. Moreover, the effects of accumulated heat stress (DHW ≥ 8 °C-weeks) on symbiont community composition appeared to be host dependent. These lines of evidence suggest that *Porites* may hold greater capacity to vary, and by extension modify, their algal symbiont community diversity than previously thought. This flexibility could contribute to the genus *Porites'* long-term evolutionary success and relative resilience to global marine heatwaves.

**Keywords** Coral reefs · Symbiodiniaceae · Marine heatwaves · Symbiosis

## Introduction

Symbiotic relationships are foundational to all ecosystems. Coral reefs exemplify this through the mutualistic interactions between scleractinian reef-building corals and the photosynthetic dinoflagellates of the family Symbiodiniaceae. These algal symbionts live within coral tissue, providing photosynthetically derived energy that supports coral growth and calcification (Muscatine 1990). In exchange, Symbiodiniaceae receive access to essential inorganic nutrients (Muscatine and D'Elia 1978). This symbiosis underpins the ecological and structural foundation of coral reefs, supporting not only the coral hosts and their algal symbionts, but also the trophic levels that depend on reef productivity (Ainsworth et al. 2010).

**Supplementary Information** The online version contains supplementary material available at https://doi.org/10.1007/s00338-026-02872-5.

✉ Lindsey Kraemer
lindsey.kraemer@my.jcu.edu.au

✉ Kate M. Quigley
katemarie.quigley@my.jcu.edu.au

1 College of Science and Engineering, James Cook University, Townsville, QLD, Australia

2 School of Molecular and Life Sciences, Curtin University, Perth, WA, Australia

3 Collections and Research, Western Australian Museum, Perth, WA, Australia

4 University of Western Australia, Perth, WA, Australia

5 The Minderoo Foundation, Perth, WA, Australia

Climate change is disrupting coral symbiosis through rising sea surface temperature (SST) and frequent accumulated heat stress events, in which SST anomalies exceed the Maximum Monthly Mean (MMM; Strong et al. 1997), often measured as Degree Heating Weeks (DHW; Gleeson and Strong 1995). This leads to coral stress, visualised as bleaching, due to the corals losing their algal symbionts (Sully et al. 2019). Prolonged, extreme temperature conditions can lead to host mortality (Hoegh-Guldberg 1999; Baker et al. 2008). The increasing frequency and intensity of these events, coupled with less stable environmental conditions (Putnam et al. 2017; Sully et al. 2019), pose a significant threat to the persistence of coral reef ecosystems by contributing to the decrease in coral cover globally (Heron et al. 2016; Hughes et al. 2018) and the loss of biodiversity and ecosystem functioning (Wernberg et al. 2024).

Corals can contend with environmental stress, including marine heatwaves, using short-term acclimatory responses or longer-term adaptive responses (reviewed by Voolstra et al. 2021). Host tolerance is influenced by its genetic makeup and the physical tolerance of its prokaryotic and eukaryotic communities (Putnam et al. 2017). Symbiodiniaceae-host associations can be specialised or generalist, where symbionts associate with multiple coral species across various environmental conditions (LaJeunesse et al. 2018). One critical acclimatory mechanism is the change in the relative abundance of Symbiodiniaceae members (shuffling) or the uptake of new symbionts from the environment (switching) (Baker et al. 2004; Quigley et al. 2022). This flexibility in diverse symbiotic associations is thought to aid in withstanding abrupt environmental stress, especially heat (Buddemeier et al. 2004; Berkelmans and van Oppen 2006; Silverstein et al. 2015; Quigley et al. 2022).

Massive growth forms of the genus *Porites* Link, 1807, can exhibit resistance to environmental stress (Levas et al. 2013). From in-situ observations across the Indo-Pacific, *Porites* colonies have demonstrated higher survival compared to other scleractinian genera (Smith et al. 2021; Terraneo et al. 2024). Along the Ningaloo Coast of Western Australia, massive *Porites* were one of the few hard coral genera to remain relatively less impacted after the 2011 mass bleaching event (Depczynski et al. 2013), as well as after a deoxygenation event that resulted in mortality across 18 other coral genera (Richards et al. 2024). Their stress tolerance is likely partly due to their thick tissue layers, slow skeletal growth, and high investment in energy reserves and cellular repair mechanisms, which together may enhance their ability to withstand thermal fluctuations, physical damage, and disease (reviewed by Putnam et al. 2017), but it is less well known if their Symbiodiniaceae communities contribute to this tolerance. The long-term paradigm is that *Porites* species generally host low-diversity communities of high-fidelity algal symbionts, particularly within the *Cladocopium* C15 lineage (LaJeunesse et al. 2004; Putnam et al. 2012). However, studies have since revealed that a broader range of symbiont associations may be possible (Ziegler et al. 2015; Pootakham et al. 2018), suggesting that *Porites* species may be more flexible in their associations than initially thought. This flexibility in their Symbiodiniaceae community composition may contribute to their relative resilience compared to other genera, like branching *Acropora* (Depczynski et al. 2013; Gardner et al. 2019), and may be a key factor in their long-term evolutionary success and stress tolerance.

The functional diversity within the Symbiodiniaceae family includes a broad range of physiological responses to environmental stress (Swain et al. 2016; Davies et al. 2023). *Cladocopium* C3, for example, is considered relatively sensitive to stress (Silverstein et al. 2015), whereas *Durusdinium* D1 is generally more stress tolerant, particularly of warming (Swain et al. 2016). However, understanding the functional diversity of Symbiodiniaceae taxa is nuanced, as physiological responses are not strictly genus-specific (Davies et al. 2023) and can vary at the intra-lineage or strain level (Howells et al. 2012; LaJeunesse et al. 2018). Both dominant and background abundances of Symbiodiniaceae are critical to determining host responses to environmental conditions (Quigley et al. 2014). Recent evidence suggests that massive *Porites* can shuffle their Symbiodiniaceae communities in response to heat stress, with some taxa becoming more prevalent following an episode of bleaching-level stress (Starko et al. 2023). Given this new insight, we sought to investigate whether Symbiodiniaceae community composition contributes to the remarkable stress tolerance exhibited by *Porites* along the mid-west coast of Western Australia in the eastern Indian Ocean (Depczynski et al. 2013; Richards et al. 2024). To do this, we examined Symbiodiniaceae community diversity within two *Porites* species within the Ningaloo World Heritage reef using high-throughput sequencing. These insights will be critical to predicting the long-term resilience of these important habitat builders along East Indian Ocean reefs.

## Methods

### Study design

The study area extended > 200 km along the Western Australia (WA) coastline from Coral Bay (23°09′15”S 113°45′56”E), to the Muiron Islands (21°40′08”S 114°21′29”E), and within Exmouth Gulf (21°52′53”S 114°11′17”E). Coral collections were made in sheltered lagoonal habitats at seven sites (see Table 1). A total of 118 *Porites* colonies were sampled via snorkel using a hammer and chisel, with ~ 8–20 colonies sampled per site (Fig. S1).

**Table 1** Sampling information and temperature metrics assessed over the climatological period 1985–2023

| Site | GPS coordinates | Marine park zoning | *Porites* colonies sampled | MMM (°C) | Annual temperature range (°C) | Warm season variability (°C) | Number of accumulated heat stress events (DHW ≥ 8 °C-weeks) | Recovery time (mean years between heat stress events) |
|---|---|---|---|---|---|---|---|---|
| MUI | 21° 40′ 40.4″ S 114° 20′ 28.9″ E | General Use | n = 20 | 28.02 | 5.30 | 0.67 | 3–6 | 6.98 |
| VLF | 21° 47′ 31″ S 114° 10′ 30″ E | Recreation/ Sanctuary | n = 20 | 27.93 | 5.24 | 0.68 | 3–6 | 6.98 |
| BUN | 21° 51′ 40.6″ S 114° 09′ 31.5″ E | Sanctuary | n = 10 | 28.00 | 5.77 | 0.68 | 3–6 | 13.95 |
| TAN | 21° 53′ 57″ S 113° 58′ 06″E | Recreation | n = 20 | 28.02 | 5.22 | 0.52 | 1–3 | 13.95 |
| LK/TR | 22° 04′ 03″ S 113° 53′ 50″ E | Sanctuary | n = 8 | 27.91 | 5.20 | 0.55 | 1–3 | 13.95 |
| OSP | 22° 14′ 34″ S 113° 49′44″ E | Sanctuary | n = 20 | 27.85 | 5.21 | 0.56 | 1–3 | 12.43 |
| COR | 23° 08′ 08.5″ S 113° 45′ 50.4″ E | Sanctuary | n = 20 | 26.78 | 4.95 | 0.63 | 6–9 | 5.15 |

The seven study sites were as follows (listed north to south): Muiron Islands = MUI, VLF Bay = VLF, Bundegi = BUN, Tantabiddi = TAN, Lakeside/Turquoise Bay = LK/TR, Osprey Sanctuary = OSP, Coral Bay = COR

To minimise contamination across samples, the chisel was cleaned with gloves to remove any existing tissue and skeletal material between colony collections. Multiple species of *Porites* (massive growth forms) were sampled at each site, including *Porites lutea* Milne Edwards & Haime, 1851 and *Porites lobata* Dana, 1846. Colonies and their respective corallites were photographed using an Olympus Tough TG-6 underwater camera to aid with ex-situ morphological assessment of each species. All sampled colonies were > 0.5 m in diameter, < 6 m in depth, and > 5 m apart from one another to minimise possible sampling of genetic clones. Fragments (< 40 mm in diameter) were chiselled at the upper-mid section of each colony. This was done to maintain consistency in morphological identification assessment and to minimise possible bias from differences in microbial composition due to intra-colony location (Lewis et al. 2022).

*Porites* colony fragments were subsampled for 1) taxonomic classification of the coral host and 2) symbiont analysis. A sterile scalpel blade was used between subsamples, focusing on scraping the central part of the sample to avoid possible external margin contamination from the chisel. Subsamples for host identification (~ 40 × 40 $mm^2$) were placed in bleach for 48 h, rinsed, and air dried for skeletal examination. Tissue subsamples for symbiont molecular studies were preserved in 100% ethanol and stored at -20 °C while at the Minderoo Exmouth Research Lab. To preserve the genetic integrity of samples, ethanol was exchanged within the first 48 h after collection. Tissue samples were then transported on ice to the Molecular Ecology and Evolution Lab (MEEL) at James Cook University (Townsville, Australia). Upon arrival, samples were topped up with 100% ethanol and stored at -20 °C until DNA extractions were performed.

Skeletal fragments of host species were examined using a Leica EZ4W stereo microscope and identified morphologically based on key diagnostic features of the calice, wall, columellae, and septal arrangement (Bernard 1905; Vaughan 1918; Pichon and Veron 1982; Budd et al. 1994). Species-level identification was determined by observations of diagnostic features and morphological descriptions of *Porites* in the Indo-Pacific, particularly those recorded from Ningaloo Reef, WA (Vaughan 1907; Pichon and Veron 1982; Veron 1985, 1986, 1993; Veron and Marsh 1988). Key characteristics used to differentiate *P. lutea* and *P. lobata* included wall thickness, septal traits (such as the fusion of the ventral triplet, length, and the number of denticles per septum), as well as the height of the pali and the morphology of the columellae (see Fig. S2). As the focus of the study was *P. lutea* and *P. lobata*, specimens identified as *Porites australiensis* Vaughan, 1918 and *Porites solida* Forskål, 1775, and specimens whose corallite features were not showing morphological characteristics of *P. lobata* and *P. lutea* were not chosen for further analysis. After specimen

identification, 44 samples were chosen for DNA extraction (Table S1). These samples included fragments identified as *P. lutea* (n = 24) and *P. lobata* (n = 13), as well as fragments that were of uncertain species—but showing morphological characteristics of *P. lobata* or *P. lutea*—requiring further analysis due to the nature of the skeletal sample collected (n = 7).

### DNA extraction, PCR amplification, and sequencing of the ITS2 region

DNA was extracted from 44 samples using the DNeasy Blood & Tissue Kit (Qiagen, USA) following the manufacturer's protocol for "Purification of Total DNA from Animal Tissues (Spin-Column Protocol)" with minor modifications (for full protocol see Data S1). PCR amplification was carried out using the multi-copy internal transcribed spacer 2 (ITS2) rDNA region, the most widely used molecular marker to resolve Symbiodiniaceae taxonomy (Davies et al. 2023). The ITS2 region (~ 350 base pairs (bp)) was amplified from the chosen 44 samples using Symbiodiniaceae-specific primers, ITS-DINO (Pochon et al. 2001) and ITS2Rev2 (Stat et al. 2009). PCR amplification was performed using procedures previously described by Quigley et al. (2022), as detailed below.

Initial PCR amplification was conducted using MyTaq DNA Polymerase (Bioline Inc.) to ensure reliable amplification of the ITS2 region from a selected DNA template (see Data S2 for protocol). For high-throughput sequencing, the ITS2 region was amplified using AmpliTaq Gold 360 Master Mix (Thermo Fisher Scientific, USA). Each 25 µl PCR included: 12.5 µl 1 × AmpliTaq Gold 360 Master Mix, 1 µl each of 0.4 µM Forward (5'- GTGAATTGCAGAACT CCGTG - 3') and Reverse (5'- CCTCCGCTTACTTAT ATGCTT - 3') primers, 9.5 µl MilliQ water, and 1 µl DNA template. PCR amplification cycles were performed on an Eppendorf Mastercycler® nexus GSX1 as follows: 95 °C for 7 min; followed by 32 cycles at 95 °C for 30 s, 57 °C for 30 s, 72 °C for 30 s, and 72 °C for 7 min. PCR products were visualised on 1.5% agarose gels. For PCR products that did not produce a visible band, template dilutions were performed (Table S1), and PCR was repeated until a clear band was confirmed by gel electrophoresis.

Library preparation and next-generation sequencing of ITS2 amplicons were completed by GenomicsWA (Perth, Western Australia). Library preparation incorporated universal Illumina adapters (Forward: 5'- TCGTCGGCAGCG TCAGATGTGTATAAGAGACAG - 3'; Reverse: 5'-GTC TCGTGGGCTCGGAGATGTGTATAAGAGACAG - 3') and PhiX genome spiking (30%). Prepared libraries were sequenced on an Illumina MiSeq platform using MiSeq Reagent Kit v2 (2 × 250 paired-end reads).

### Bioinformatics

Sequenced reads were demultiplexed using provided index information and Illumina's bcl2fastq program (Illumina 2017). The BBTools program 'BBduk' (http://sourceforge.net/projects/bbmap/) was used to remove index sequences and residual Illumina adapter content. FastQC and MultiQC were used to assess sequence quality and confirm the absence of adapter contamination. Following this, all downstream analyses were performed in R (version 4.1.2; R Core Team 2021).

Amplicon analysis is necessary for the removal of errors introduced during high-throughput sequencing. The multicopy nature of the ITS2 region means that single nucleotide differences can be biologically significant or genetically trivial when resolving taxonomic boundaries and assessing ecological functions (Quigley et al. 2014; Davies et al. 2023). Clustering sequences based on similarity thresholds can limit noise introduced by intragenomic variants (Arif et al. 2014; Ziegler et al. 2018) and inform functional diversity metrics by mapping to known ancestral haplotypes and sub-types (Correa and Baker 2009; Hume et al. 2019); however, this also means that taxonomic resolution can be coarse, potentially leading to underestimates of biodiversity (Cunning et al. 2017). Hence, for exploring potentially novel diversity, it is critical to employ high specificity during the denoising process to aid in taxonomic delineation and abundance estimates. The "DADA2" package uses a statistical model-based approach in error detection that allows for improved resolution of sequence variants relative to that of OTU-clustering methods (Callahan et al. 2016).

A standard amplicon analysis workflow was performed using "DADA2" (version 1.22.0; Callahan et al. 2016) with modifications specifically for Symbiodiniaceae (Quigley et al. 2019). Briefly, raw (demultiplexed, adapter-trimmed) reads were first filtered based on read quality scores (Phred score > 30), and then by the "DADA2" error modelling algorithm. Forward and reverse reads were then merged, filtered, and amplicon sequence variants (ASVs) were inferred. Although "DADA2" promotes inclusion of subtle yet potentially meaningful genomic differences, it is still crucial to check for possible overestimation of biodiversity. The "LULU" pipeline (version 0.1.0; Frøslev et al. 2017) collapses any intragenomic variants that are likely to represent the same 'genotype,' if present. "LULU" was run on curated ASVs, using both default (95%, 84%) and conservative (70%, 84%) threshold criteria for sample co-occurrence and sequence similarity, respectively (Quigley et al. 2019).

Biologically relevant variants were then taxonomically classified using the RDP Naïve Bayesian Classifier algorithm (Wang et al. 2007) implemented in "DADA2" aligned to a custom database of ITS2 sequences linked to known taxonomy (Arif et al. 2014). A separate BLAST of curated

ASVs was run against the reference database to ensure that identities matched. For variants that did not map to the reference database, a nucleotide BLAST search was conducted using the BLAST + 2.15.0 suite against the NCBI nucleotide collection (nt) database (Table S2; Camacho et al. 2009). The search parameters were set to an expected value (E value) threshold of 1e-5, match/mismatch of 1, -2, and gap-costs of 0, 2.5 to ensure high confidence in alignments (hits).

### Read depth, intragenomic variation, and taxonomic assignment

A total of 19,075,730 sequenced reads were recovered from the 44 samples sent for Illumina sequencing. The mean sequencing depth was 216,770 ± 3,618 reads per sample. All values are reported as mean ± standard error (SE) unless otherwise stated. Pre-processing steps removed 0.1% of reads, leaving 18,901,656 reads for input into "DADA2" for amplicon analysis (mean 211,304 ± 5,018 reads per sample). During chimera identification in the "DADA2" workflow, 2,304 of the 3,489 inferred sequence variants (within the expected range of 294 to 304 bp in length) were identified as chimeras. After bioinformatic processing and chimera removal through the "DADA2" pipeline, a total of 8,065,014 paired reads (94.7%; mean 183,296 ± 4,525 reads per sample) mapped to the remaining 1,185 ASVs across all 44 *Porites* samples (Table S1). The "LULU" algorithm did not collapse and merge any ASVs in this dataset in either case where co-occurrence and sequence similarity thresholds were set at default criteria (95% and 84%, respectively) or conservative criteria (70% and 84%, respectively). Hence, previous filtering steps had identified and removed intragenomic variants. Given this, the full, cleaned dataset of 1,185 ASVs was retained and imported into "phyloseq" (version 1.46.0; McMurdie and Holmes 2013) for further analysis.

156 of 1,185 ASVs (13.2%) were not mapped to known ITS2 taxonomic identifications within the reference database. Our BLAST search yielded more than 300 significant hits for each of the 156 unclassified variants. All hits were within the family Symbiodiniaceae. Sub-genus-level classification was determined based on the accession match with the highest score for percentage identity (≥ 98%) and the lowest E value (minimum E value: 1e-140; Table S2)**.** In cases of multiple hits to sub-genus taxa with the same score and E value, classified ASVs were named in the order of the appearance of hits (i.e. "C91_C15**").** Thus, all 1,185 ASVs retrieved from this dataset were identified using the reference database or manual BLAST searches.

Further analysis included only samples morphologically identified as *P. lutea* (n = 24) and *P. lobata* (n = 13) (see Fig. S2). There were a total of 6,833,662 total reads mapping to 1,001 ASVs remaining within these 37 samples. On average, sequencing depth was 184,694 ± 4,947 reads per sample, ranging from a minimum of 110,476 reads to a maximum of 267,804 reads (Table S3). Rarefaction curves of untransformed data were assessed to ensure sequencing depth was sufficient to capture ASV diversity across samples (Fig. S3). Rarefaction curves were generated using the 'rarecurve' function from the "vegan" package (version 2.6–4; Oksanen et al. 2022).

### Temperature metrics

To examine the relationship between Symbiodiniaceae community composition and historical temperature metrics, sea surface temperature (SST) data were sourced from the NOAA Coral Reef Watch (CRW) Climatology and Stress Frequency databases (version 3.5; Heron et al. 2014; Skirving et al. 2020). For each site, data were extracted for the following temperature metrics over the climatological period 1985–2023. Maximum Monthly Mean (MMM), defined as the long-term mean SST for the warmest month of the year (°C), reflects the upper boundary of typical thermal conditions that corals historically experience at a given location. Annual temperature range (°C; hereafter referred to as temperature range), defined as the difference between the warmest and coolest monthly mean SSTs, provides an estimate of the typical thermal range experienced at each site. Warm season variability (°C), defined as the interannual standard deviation of daily SSTs over the three-month period encompassing the climatological warmest month, captures year-to-year fluctuations in peak seasonal temperatures. The number of accumulated heat stress events, defined as the summed number of severe bleaching-level heat stress events with DHW ≥ 8 °C-weeks, quantifies the frequency with which sites experienced extreme episodes of thermal disturbance over the climatological period (1985–2023). The final metric derived, recovery time, captures the mean time interval (in years) between episodes of severe bleaching-level heat stress. These temperature metrics were derived from 5 km-resolution satellite time series products in NetCDF4 format (NOAA Coral Reef Watch 2024). Data were processed and visualised in R (version 4.1.2; R Core Team 2021) using the "ggplot2" (version 3.5.1; Wickham 2016), "ggspatial" (version 1.1.9, Dunnington et al. 2023), and "sf" (version 1.0.16; Pebesma 2018) packages.

### Statistical analyses

ASVs, sample metadata, and taxonomic classifications were imported into "phyloseq" to test for patterns within and across Symbiodiniaceae communities from the *Porites* samples chosen for further analysis (n = 37; Table S3). The "ape" package (version 5.8; Paradis et al. 2004) was used to construct a phylogenetic tree so that ASV phylogenetic relationships could be incorporated into downstream analysis.

Normalisation and transformation were performed on raw reads using tools from the "microbiome" package (version 1.24.0; Lahti and Shetty 2017) and "DESeq2" package (version 1.42.1; Love et al. 2014). Standard deviation plots were used to evaluate the most appropriate transformation method (Anderson et al. 2006), and variance stabilising transformation (VST) was selected as the best fit for this dataset (Fig. S4). All analyses, except for alpha diversity, used normalised and VST abundance data.

To account for both abundance data and phylogenetic relationships between ASVs, weighted UniFrac distances were generated from normalised read counts. These distances represent beta diversity, quantifying differences in Symbiodiniaceae community composition between samples or groups, where groups were defined based on tested factors (i.e. host species, site, temperature metrics) (Lozupone et al. 2007). A non-metric multidimensional scaling (NMDS) ordination was performed on the resulting distance matrix to visualise differences in Symbiodiniaceae communities across tested factors (host species and temperature metrics; see Fig. S5 for stress plot). To assess whether dispersion (within-group variability) of symbiont communities differed across factors, we applied a Homogeneity of Dispersion analysis (PERMDISP) using the 'betadisper' and 'permutest' functions in the "vegan" package (Table S4). The 'betadisper' function was used to calculate the distance from each sample to its group centroid, and permutation-based ANOVA ('permutest') was used to test for differences in mean dispersion among groups. Because sample sizes differed among host species across sites, the bias.adjust = TRUE parameter was applied to reduce potential bias in centroid estimation. Prior to PERMANOVA, collinearity among explanatory variables (temperature metrics, latitude, and longitude) was assessed using pairwise Pearson correlation analyses (Fig. S6, Table S5). Highly correlated variables ($|r| > 0.7$) were not included together in the same models to avoid redundancy and inflation of explained variance. To evaluate the individual and interactive effects of host species, site, and temperature metrics on symbiont community composition (beta diversity), we performed permutational multivariate analysis of variance (PERMANOVA; Anderson 2017) using the 'adonis2' function with 999 permutations (Tables S6, S7).

While NMDS, PERMDISP, and PERMANOVA assessed community-level patterns, differential abundance analysis was conducted to identify specific ASVs contributing to observed differences. Differential abundance testing was performed on models that included statistically significant factors and interactions using the "DESeq2" package. A negative binomial generalised linear model (GLM) was fit to raw count data using the 'DESeq' function with the parameter 'fitType' set to "local" (Fig. S7). Wald tests were used to assess the significance of differences in ASV abundance, with Benjamini–Hochberg adjusted p-values set to a 5% false discovery rate. Shrunken $\log_2$ fold changes were estimated using the 'apeglm' method to obtain stable effect size estimates (Zhu et al. 2019).

Transforming count data prior to quantifying alpha diversity can lead to a misrepresentation of biologically meaningful variance (McKnight et al. 2019), and rarefaction can discard robust data and reduce statistical power when sequencing depth is sufficient (McMurdie and Holmes 2014). Hence, because rarefaction curves across all samples indicated adequate sampling depth (Fig. S3), alpha diversity metrics were calculated using untransformed count data. Shannon's Diversity Index ($H'$) and the Gini-Simpson index ($1 - D$) were used to assess species richness and evenness of Symbiodiniaceae communities across categorical factors (Table S8). Prior to statistical comparisons, data were tested for normality (Shapiro–Wilk Test; Fig. S8, Table S9) and homoscedasticity (Levene's Test; Table S10) using the "car" package (version 3.1.2; Fox and Weisberg 2019). Depending on data distribution, differences in alpha diversity among groups were evaluated using independent *t*-tests or Welch's ANOVA (Tables S11, S12).

## Results

### Temperature metrics vary across sites

The reef sites where corals were sampled exhibited distinct patterns across different sea surface temperature (SST) metrics, the number of accumulated heat stress events, and recovery time post-heat stress (Fig. 1, Table 1, File S1). All values are reported as mean ± standard error (SE) unless otherwise stated. Maximum Monthly Mean (MMM) temperatures followed a latitudinal gradient (Fig. S9a), with the southernmost site (Coral Bay = COR) exhibiting the lowest mean temperature (MMM = 26.78 ± 1.85 °C), whilst the northernmost site (Muiron Islands = MUI) was the warmest (MMM = 28.02 ± 2.04 °C). The site located within the Exmouth Gulf (Bundegi = BUN) exhibited the largest temperature range (5.77 ± 0.62 °C) compared to the six other sites (Fig. S9b). For the six sites outside of Exmouth Gulf, mean temperature range decreased with latitude (range: 4.95 ± 0.53 °C—5.30 ± 0.59 °C). Warm season variability was lowest at central sites (Osprey Sanctuary = OSP, Lakeside/Turquoise Bay = LK/TR, Tantabiddi = TAN; < 0.57 ± 0.13 °C), compared to greater variability during the warmest part of the year at the northern and southern extremes of the sampling range (MUI, VLF, BUN, COR; 0.63–0.68 ± 0.13 °C; Fig. S9c). The history of heat stress also varied spatially (Fig. 1), with the southernmost site (COR) experiencing the greatest number of

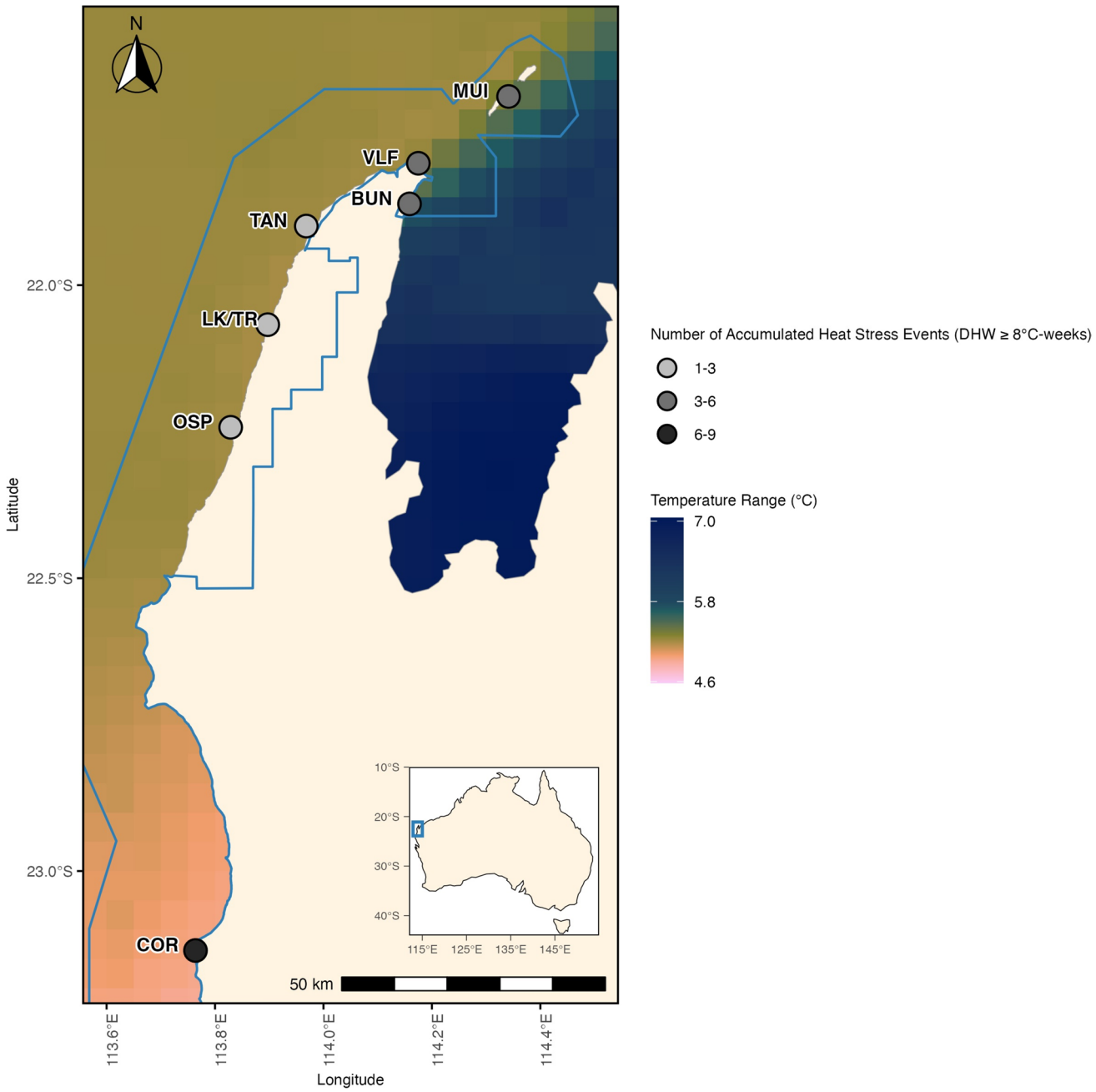


**Fig. 1** Spatial variation in key temperature metrics across sampled sites along World Heritage-listed Ningaloo Reef, Western Australia. The temperature metrics depicted here include annual temperature range (°C; less in pink to greater in dark blue) and the number of accumulated heat stress events (DHW ≥ 8 °C-weeks) per site. Circular datapoints at study sites correspond to the following: 1–3 events (light grey), 3–6 events (grey) and 6–9 events (dark grey). Blue lines indicate UNESCO World Heritage Ningaloo Coast boundaries (UNESCO 2023). The inset map (bottom right) highlights the location of Ningaloo Reef within Australia

accumulated heat stress events (n = 6–9 events; defined as DHW ≥ 8 °C-weeks) and the shortest recovery time between events (mean 5.15 ± 0.35 years; Table 1). Northern sites (MUI, VLF, BUN) experienced an intermediate number of accumulated heat stress events (n = 3–6 events), and recovery time ranged from 6.98 ± 0.60 years to 13.95 ± 1.21 years. Sites with the lowest number of accumulated heat stress events included the central sites (OSP, LK/TR, TAN; n = 1–3 events), which also recorded recovery times exceeding > 12 years (Table 1, File S1).

### Symbiodiniaceae community composition and correlation with host species and temperature metrics

Acknowledging the complexity of Symbiodiniaceae taxonomy (see Davies et al. 2023 for a full discussion), groups of similar Amplicon Sequence Variants (ASVs) are described herein as "taxa" for simplicity, though they may not represent formally recognised taxonomic units. A total of 1,001 ASVs were mapped to 25 taxa within the genus *Cladocopium* across all coral samples. Overall, Symbiodiniaceae communities were dominated by C15, which accounted for 708 of the total ASVs. In terms of prevalence throughout the dataset, C15 was followed by C15h (35 ASVs), C116 (49 ASVs), and C15.9 (29 ASVs), with the remaining 180 ASVs belonging to other *Cladocopium* taxa (Fig. S10).

The prevalence of different *Cladocopium* taxa and their normalised relative abundance varied across host species and sites (Fig. 2). Specific *Cladocopium* taxa were uniquely associated with each host species (File S2). For example, C15f and C91b were only detected in *P. lobata* samples, whereas C15g, C15i, C15d were only detected in *P. lutea* samples (Table S13). Moreover, specific taxa were unique to certain sites (C15.1 was only detected in BUN, C91a in COR, C15j and C50 in MUI), while other taxa were absent in other sites (e.g., C116 and C15.8 were not present in LK/TR and OSP, or BUN, respectively; Fig. 2, Table S13).

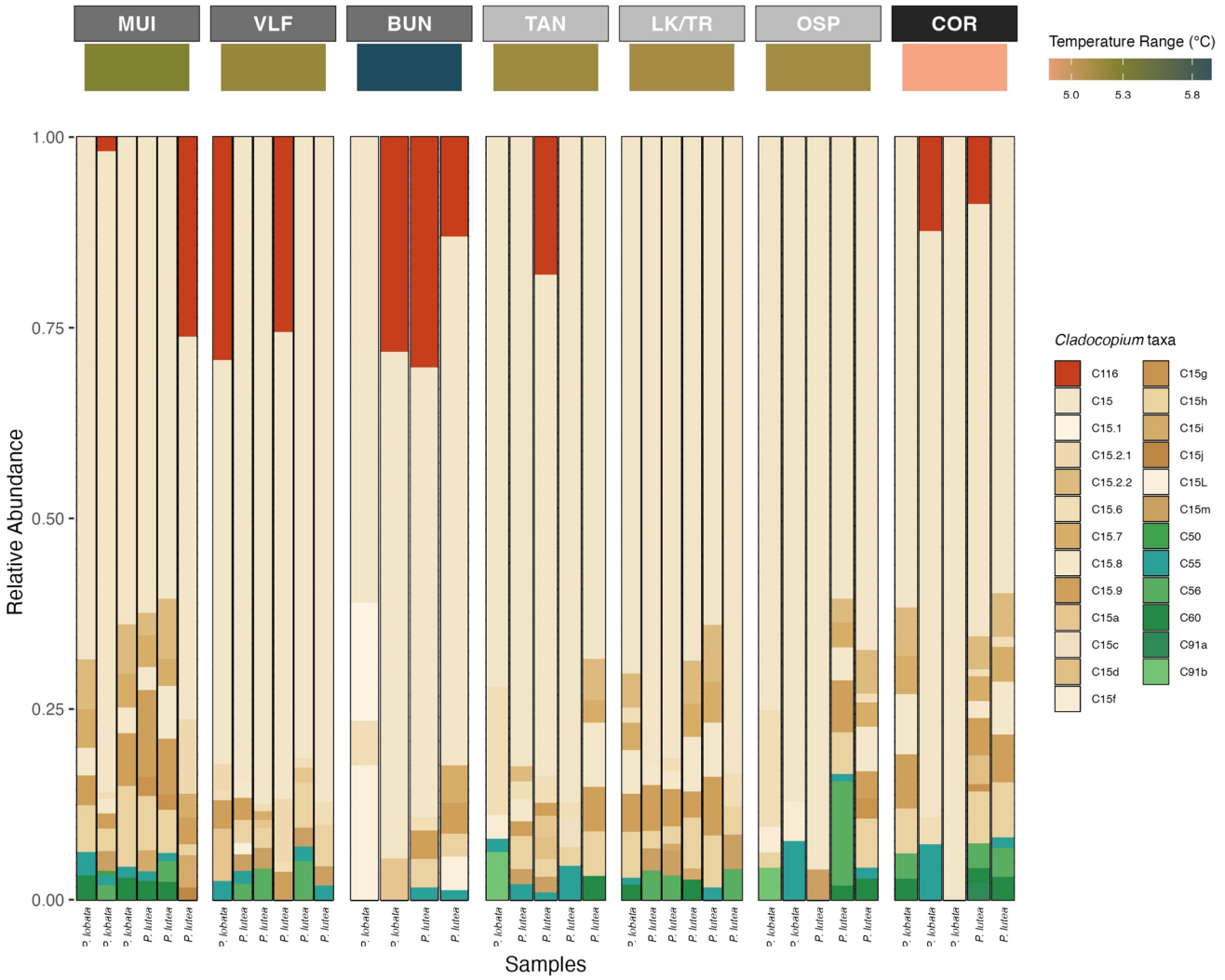


**Fig. 2** Normalised relative abundances of *Cladocopium* taxa across samples. Each bar represents a *Porites* coral sample. Different colours within each bar represent the *Cladocopium* taxa detected in each coral sample. Each bar is labelled by host species (bottom). Facets are representative of study sites and are arranged from north to south (from left to right), with the Muiron Islands (MUI) as the northernmost site. Site labels, in grey-scale, correspond to the number of accumulated heat stress events (DHW ≥ 8 °C-weeks) per site (1–3 events (light grey), 3–6 events (grey) and 6–9 events (dark grey)). The colour beneath each site label indicates the annual temperature range experienced at that site (temperature range °C; less in pink, to mid in green, to greater in blue)

Certain *Cladocopium* taxa were ubiquitous across all sites and host species (Fig. 2, Table S13). C15 was detected across all samples and sites, comprising 89.0 ± 1.6% of the relative abundance of ASVs per sample (Tables S3, S12). C15h, the second most prevalent *Cladocopium* taxon, was detected in 28 of 37 samples, with a mean relative abundance of 0.7 ± 0.1% per sample (Table S14). C15h occurred more frequently in *P. lutea* than in *P. lobata* (92% versus 46% of samples; File S2). It was detected across all sites and was most prevalent at the warmest site (highest MMM, MUI, 100% of samples; Fig. 2, File S2), whereas at the site with the greatest temperature range (BUN), it was present in 50% of samples. Another common taxon, C15.9, was detected in 24 samples and had a mean relative abundance of 1.4 ± 0.2% per sample (Table S14). C15.9 also occurred more frequently in *P. lutea* than in *P. lobata* (75% versus 46% of samples; File S2). It was most prevalent at the warmest site (MUI, 100% of samples) and was detected in over 40% of samples across all sites (File S2).

Of the observed Symbiodiniaceae taxa, 28% (7 of 25) of the *Cladocopium* were not identified to C15. Six of these seven taxa were in low abundance (≤ 1%; Table S14). C116 was the exception, occurring in 10 of the 37 samples, with a mean relative abundance of 12.6 ± 3.0% across samples (Table S14, File S2). C116 was detected across both host species and five sites (Fig. 2). It was most prevalent at the site with the largest temperature range (BUN), where it comprised 13–30% of the relative abundance per sample in 75% of samples (Fig. 2). At the site with the smallest temperature range and greatest number of accumulated heat stress events (COR), C116 accounted for > 10% of the relative abundance in 40% of samples (Table S3, File S2). C116 was uncommon or absent at sites experiencing the lowest number of accumulated heat stress events (TAN, LK/TR, OSP; Fig. 2). Several low-abundance *Cladocopium* taxa were broadly distributed across sites and host species. C55 was present in 22 of 37 samples, with a mean relative abundance of 0.3 ± 0.1%, occurring in 62% of *P. lobata* and 58% of *P. lutea* samples (Table S14, File S2). It was most prevalent at the warmest sites (MUI and TAN, ~ 80% of samples) and commonly co-occurred with C15.9 and/or C15h (19 samples; Table S3). C56 (1.3 ± 0.6%) and C60 (0.3 ± 0.1%) were detected in 12 samples across five sites (Tables S13, S14). Both taxa occurred more frequently in *P. lutea* (42% and 33%, respectively) than in *P. lobata* samples (15% and 31%, respectively), and were most prevalent at the site with the smallest temperature range and the greatest number of accumulated heat stress events (COR, ~ 60% of samples). Neither C56 nor C60 were detected at the site with the largest temperature range (BUN; Table S13).

Overall, *Cladocopium* community composition exhibited spatial structuring and was correlated with subsets of metrics, including host species, temperature range, and number of accumulated heat stress events (Figs. 2, 3). Weighted UniFrac-based PERMANOVA indicated that Symbiodiniaceae community composition varied significantly with host species and temperature range (Tables S6, S7). In single-factor models, host species explained 6.8% of variation in community composition ($F = 2.560$, $R^2 = 0.068$, $p = 0.048$), while temperature range explained 10.8% ($F = 4.245$, $R^2 = 0.108$, $p = 0.010$). In contrast, other metrics (number of accumulated heat stress events, MMM, warm season variability, recovery time, longitude), did not significantly explain variation as a single factor (PERMANOVA: $p > 0.05$; Table S7).

Pearson correlation analyses indicated that some of the tested variables were moderately to highly correlated (Fig. S6, Table S5), particularly latitude and maximum SST ($r = 0.959$). In the main multivariable model (Table S6), host species ($F = 3.272$, $R^2 = 0.078$, $p = 0.022$) and temperature range ($F = 2.693$, $R^2 = 0.065$, $p = 0.043$) remained significant predictors of symbiont community composition, whereas the number of accumulated heat stress events did not explain additional variation after accounting for these factors (PERMANOVA: $p > 0.05$; Table S6). Together, host species and temperature range explained approximately 14% of the variation in Symbiodiniaceae community composition.

Tests of multivariate dispersion showed that community dispersion differed significantly between host species (PERMDISP: $F = 6.303$, $p = 0.027$), with greater mean distance to centroid in *P. lobata* (0.390) than in *P. lutea* (0.245), indicating greater within-host variability in *P. lobata* communities (Figs. 3, S11, Table S4). In contrast, dispersion did not differ significantly among sites or the number of accumulated heat stress events (PERMDISP: $p > 0.05$; Table S4). Because host representation varied among sites, a stratified PERMANOVA with permutations constrained within site was also performed. Host species remained a significant predictor of symbiont community composition under this restricted permutation scheme ($F = 2.560$, $R^2 = 0.068$, $p = 0.032$; Table S7). Interaction models indicated that the relationship between the number of accumulated heat stress events and symbiont community composition differed between host species (host × DHW: $F = 3.609$, $R^2 = 0.157$, $p = 0.007$; Table S6), explaining 15.7% of variation in community composition. By contrast, the interaction between the number of accumulated heat stress events and temperature range was not significant (DHW x temp. range: $p > 0.05$; Table S6).

These patterns were visualised in NMDS ordinations, where samples clustered along the temperature range gradient (Figs. 3a, S12). Host-specific structuring within accumulated heat stress categories was also present in faceted ordinations (Fig. 3b). Notable clustering included samples from sites experiencing an intermediate number of accumulated heat stress events (3–6 events; NMDS—bottom right; Figs. 3, S13); all of which included the same five

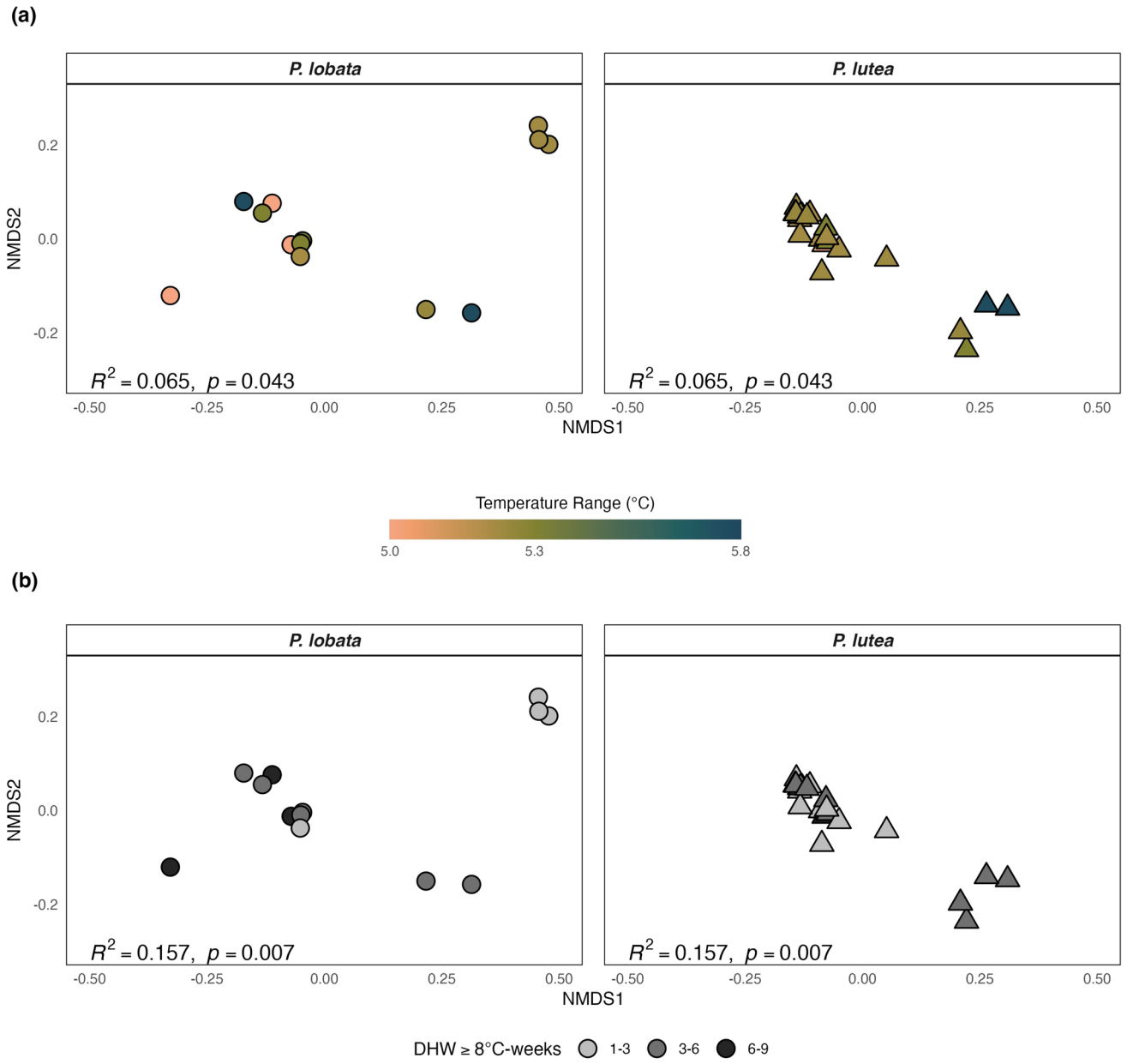


**Fig. 3** Non-metric multidimensional scaling (NMDS) of Symbiodiniaceae community composition based on weighted UniFrac distances (stress = 0.041). Points represent unique Symbiodiniaceae communities associated with individual *P. lobata* (circles) and *P. lutea* (triangles) samples. Symbiodiniaceae community dispersion and structure were significantly different between host species (Homogeneity of Dispersions: $F = 6.303$, $p = 0.027$; PERMANOVA: $F = 3.272$, $R^2 = 0.078$, $p = 0.048$). Communities are coloured by (**a**) temperature range (°C; PERMANOVA: $F = 2.693$, $R^2 = 0.065$ $p = 0.043$), and (**b**) number of accumulated heat stress events (DHW ≥ 8 °C-weeks; host x DHW PERMANOVA: $F = 3.609$, $R^2 = 0.157$, $p = 0.007$)

ASVs mapping to C116 (ASV11, ASV12, ASV28, ASV29, ASV96; File S2). *P. lobata* samples from sites experiencing the lowest number of accumulated heat stress events (1–3 events; NMDS—top right; Figs. 3, S13) were the only samples to share ASVs mapping to C15f (ASV235, ASV280; File S2). One *P. lobata* sample from the site with the highest number of accumulated heat stress events (6–9 events; NMDS—bottom left; Figs. 3, S13) was the only sample in which the symbiont community composition was made up of entirely C15 (12 ASVs mapping to C15; Fig. 2, File S2).

To identify *Cladocopium* taxa driving community-level differences between host species, differential abundance analysis was performed using an additive model including host species, the number of accumulated heat stress events, and the temperature range (Fig. 4, File S2). Comparisons between host species revealed both taxon-level

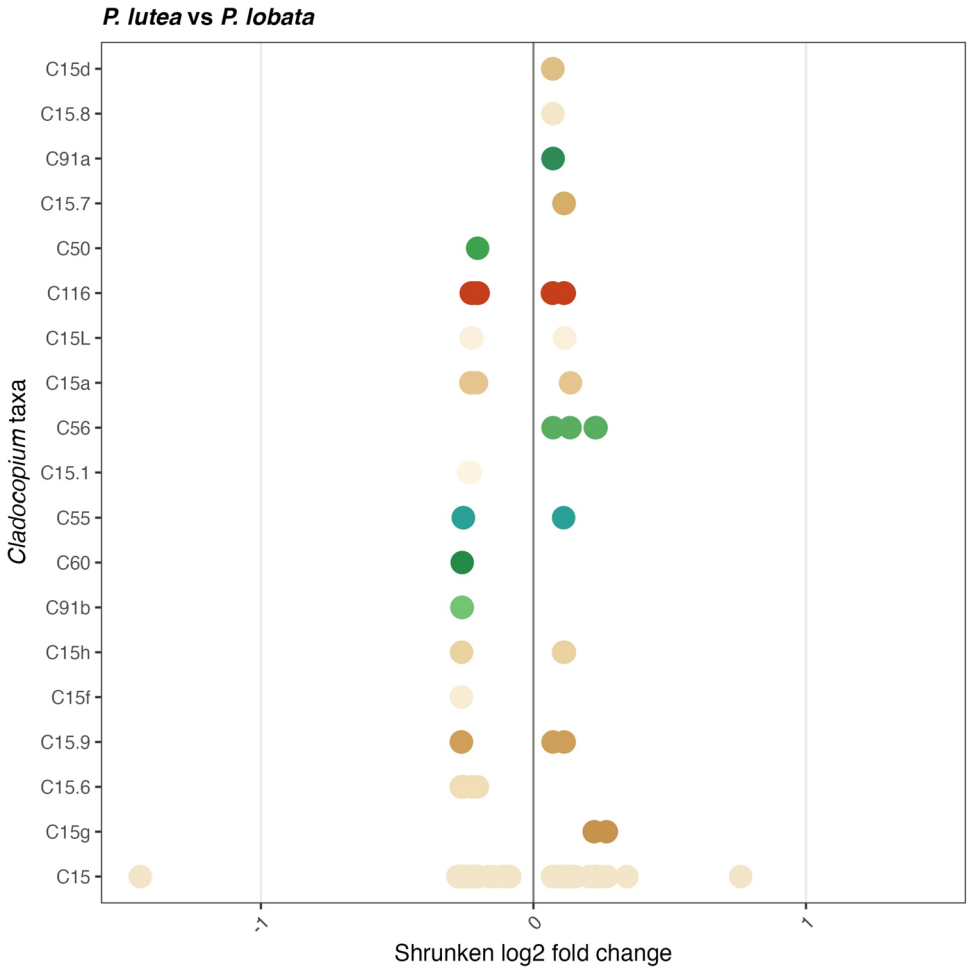


**Fig. 4** Differential abundance of *Cladocopium* taxa between host species. Points represent individual amplicon sequence variants (ASVs) assigned to *Cladocopium* taxa (y-axis) that were significantly differentially abundant (adjusted $p < 0.05$; DESeq2). $Log_2$ fold changes (x-axis) are shown as shrunken effect size estimates (method: 'apeglm'), where positive values indicate higher abundance in *P. lutea* and negative values indicate higher abundance in *P. lobata*. The model accounts for number of accumulated heat stress events (DHW > 8 °C-weeks) and temperature range. Multiple points presented per *Cladocopium* taxa represent multiple significantly differentially abundant ASVs identified within each taxa

and within-taxon host specificity of symbionts ($log_2$ fold change, adjusted $p < 0.05$; Table S15). Several *Cladocopium* taxa exhibited consistent host associations, including C15.6 and C91b, which were exclusively enriched in *P. lobata*, and C56, C15d, C15g, and C91a, which were enriched in *P. lutea*. In contrast, the dominant *Cladocopium* taxa C15, as well as C116, displayed mixed host associations, with ASVs within each taxon enriched in both host species (Fig. 4). For example, 197 C15 ASVs were differentially abundant (adjusted $p < 0.05$; File S2), with 82 enriched in *P. lutea* and 115 in *P. lobata* (Table S15).

To investigate taxa underlying the significant host species × heat stress categories interaction detected in PERMANOVA (see Table S6), differential abundance analysis was performed using a separate interaction model including host species, the number of accumulated heat stress events, and their interaction (File S2). Although the interaction was statistically significant (PERMANOVA: $F = 3.609$, $R^2 = 0.157$, $p = 0.007$; Table S6), DESeq2 results indicated that it was driven by subtle ASV-level shifts rather than large abundance changes in individual taxa (File S2). Interaction-associated signal was concentrated in a small number of taxa, particularly within the dominant C15 lineage, but shrunken effect sizes were uniformly small (shrunken $log_2$ fold change values ~ $10^{-7}$; Table S16, File S2).

## Site-level patterns are exploratory

Exploratory PERMANOVA indicated that symbiont community composition differed among sites ($F = 1.728$, $R^2 = 0.257$, $p = 0.037$; Fig. S12, Table S7). However, site-level results were interpreted cautiously because host species replication within sites was limited. Site patterns were therefore used primarily to provide ecological context for environmental gradients and differential abundance patterns, rather than as a primary inferential result.

## Sequence diversity within Symbiodiniaceae communities

To further explore sequence-based diversity, two alpha diversity metrics were calculated on raw count data using categorical factors (host species, site, and number of accumulated heat stress events). These metrics included Shannon's

Diversity Index (hereafter referred to as richness; *H'*) and the Gini-Simpson index (hereafter referred to as evenness; 1-*D*). Across all tested factors, trends in these metrics were present but not statistically significant (independent t-test, $p > 0.05$; Welch's ANOVA, $p > 0.05$; Tables S11 and S12). Richness was greater in *P. lutea* compared to *P. lobata* ($H' = 2.27 \pm 0.09$ vs. $2.12 \pm 0.14$), whereas evenness was similar in *P. lobata* compared to *P. lutea* ($1\text{-}D = 0.77 \pm 0.03$ vs. $0.77 \pm 0.02$; Fig. S13a, Table S8). Richness was lowest at the coolest sites (COR, $H' = 2.05 \pm 0.19$) and highest at the sites of highest MMM (MUI, $H' = 2.44 \pm 0.17$; Fig. S14a, Table S8). Evenness was lowest at the most central site (LK/TR, $1\text{-}D = 0.75 \pm 0.03$) and highest at the warmest site (MUI, $1\text{-}D = 0.80 \pm 0.03$; Fig. S14b). Sites with an intermediate number of accumulated heat stress events (3–6 events) exhibited the highest richness and evenness ($H' = 2.29 \pm 0.14$ and $1\text{-}D = 0.79 \pm 0.03$; Fig. S14c, Table S8). Sites with the highest number of accumulated heat stress events (6–9 events) had the lowest richness ($H' = 2.05 \pm 0.19$) and sites with the lowest number of accumulated heat stress events (1–3 events) had the lowest evenness ($1\text{-}D = 0.76 \pm 0.02$; Fig. S14c).

## Discussion

This study provides novel insights into the diversity and distribution of Symbiodiniaceae communities in massive *Porites* species (*P. lutea* and *P. lobata*) along the Ningaloo Coast World Heritage reef in Western Australia. We found that both host identity and historic thermal variability in SST contribute to differences in symbiont community composition, while the effects of accumulated heat stress events (DHW ≥ 8 °C-weeks) appear to be host dependent.

Host identity emerged as a primary driver of symbiont community structure. Community composition differed significantly between *P. lutea* and *P. lobata*, and this pattern remained significant even when permutations were constrained within site, indicating that host-associated differences were not solely driven by geographic variation. These differences could be driven in part by host genetics (Starko et al. 2023; Grupstra et al. 2024), could be an emergent property of differences in physiological traits like tissue thickness (Putnam et al. 2017), or could be attributed to something else. As the sample size in this study was relatively limited, further research is encouraged to assess this. *P. lobata* communities exhibited greater dispersion than those of *P. lutea*, suggesting higher among-colony variability in symbiont assemblages, as was visualised in ordination space. Differential abundance analysis further supported these patterns, with multiple taxa enriched in one host relative to the other.

Interestingly, while *Cladocopium* C15 was the dominant symbiont across most samples, substantial ASV-level diversity was retained within this taxonomic group. Differential abundance analysis revealed significant enrichment of different ASVs mapping to C15 for each host species, highlighting that host-specific structuring of Symbiodiniaceae communities may occur not only at the taxon level but also among closely related sequence variants within taxa. We also recovered substantial diversity among C15-associated ASVs (like C15h, C15.9, C15L), each present at varying abundances across samples. Although Symbiodiniaceae taxonomy is under active revision (Davies et al. 2023), this diversity may reflect the presence of distinct lineages within the broader C15 group. While $\log_2$ fold change was minor for the differential abundance analysis based on host x heat stress interaction, host species exhibited a stronger change in abundance of ASVs mapping to several of these background *Cladocopium* taxa with a change in the number of accumulated heat stress events (see Table S16). This pattern supports growing evidence that Symbiodiniaceae diversity within *Porites* is not limited to a single stable lineage, but instead includes multiple closely related variants, and more, that may differ in ecological function or environmental tolerance (Starko et al. 2023). Differences in symbiont community structure between these two host species may reflect differences between *P. lutea* and *P. lobata* in terms of their ecological niches or strategies for coping with environmental stress (Grupstra et al. 2024).

Annual temperature range in SST influenced symbiont community composition, remaining a significant predictor in both single-factor and multivariable PERMANOVA models. Sites experiencing greater temperature range or more frequent thermal stress (such as Bundegi and Coral Bay) harboured higher abundances of thermotolerant *Cladocopium* taxa, notably C116 (Tonk et al. 2014; Swain et al. 2016). In contrast, at historically thermally stable sites (Lakeside/Turquoise Bay, Osprey Sanctuary), C116 was either present in low abundance or absent altogether. The presence and repeated occurrence of C116 at warmer, more thermally variable, and more disturbed sites suggest that it may be a heat-associated symbiont in this system, becoming abundant in response to thermal stress. This has been observed in other locations around the world (Pootakham et al. 2018; Starko et al. 2023). Moreover, the observed difference of ASVs mapping to C116 at sites with varying accumulated heat stress (3–6 events versus 6–9 events), and variation in enriched ASVs mapping to C116 in *P. lutea* versus *P. lobata* samples, further indicate that intra-taxonomic diversity may play a role in host-specific responses to thermal stress. This change in distribution may reflect environmental filtering or potential local adaptation to varying temperature conditions observed across our study sites, as has been observed in other studies around the world (Arif et al. 2014; Claar et al. 2020). Together, these patterns of presence, absence, and ASV-level variation suggest that C116 may contribute

to the resilience of massive *Porites* in locations exposed to recurrent heat stress.

In addition to dominant taxa, a range of background taxa, including C60, C55, and C91b, was detected across samples. Although present at low abundance, several of these background *Cladocopium* taxa were significantly enriched across differential abundance analyses testing the effect of host and the interaction of host x heat stress, indicating that these taxa may contribute to additional functional diversity within the holobiont. The trend of detecting additional diversity within *Porites* species is growing with improved sequencing tools (see Claar et al. 2020). While the ecological roles of these background taxa are not fully understood, increasing evidence suggests that background symbionts can provide functional redundancy, enhancing holobiont stability under differing environmental conditions (Ziegler et al. 2018).

Site-level differences were detected in exploratory analyses, but given uneven and limited host replication across sites, this factor is better interpreted as ecological context rather than a primary inferential factor. Several explanatory variables, including latitude and MMM, were correlated, indicating that broad-scale thermal regimes likely underpin observed spatial patterns in symbiont community composition. For example, clustering patterns from *P. lutea* and *P. lobata* samples at the northernmost sites (see Fig. S13) may be explained by the greater annual temperature range in these locations or the increased accumulation of heat stress at these sites. The annual temperature range is likely influenced by the diurnal tidal currents within Exmouth Gulf, which might also play a role in driving similarities between sites in in-hospite symbiont communities. Aside from the temperature-related metrics examined here, additional unmeasured environmental factors (e.g., hydrodynamics, connectivity) may also play a role in influencing symbiont community structure (Vanderklift et al. 2020), aligning with previous findings for massive *Porites* (Tan et al. 2020). Further investigation is encouraged.

These findings challenge the long-standing view that massive *Porites* host uniformly stable, low-diversity algal symbiont communities dominated by a single *Cladocopium* C15 lineage (Putnam et al. 2012). Instead, our results here and others (Qin et al. 2019) show that *Porites* species exhibit greater symbiont flexibility and diversity than previously assumed (Terraneo et al. 2024). This may be contributing to their resistance to thermal stress. Indeed, the ability to adjust the relative abundance of existing symbionts ("shuffling") or to acquire new symbiont types ("switching") is a common mechanism corals use to cope with environmental stress (Baker 2003; Quigley et al. 2022). The detection of thermally tolerant taxa like *Cladocopium* C116 suggests that *Porites* may have greater capacity than initially thought to shuffle or switch in response to heat stress or differences across the environment (Starko et al. 2023). Importantly, the strongest signal in this dataset lies in community composition and taxon-specific abundance shifts rather than alpha diversity richness and evenness, which showed trends across host species, sites, and heat stress categories but were not statistically significant. This suggests that symbiont flexibility in massive *Porites* could be expressed primarily through compositional restructuring rather than large shifts in within-sample diversity.

Given the increasing frequency and severity of marine heat waves globally, understanding how coral-symbiont associations respond to environmental variability is critical. Our study highlights previously undetected diversity and flexibility in Symbiodiniaceae communities hosted by massive *Porites* species along the Ningaloo Coast. Continued monitoring and experimental work will be essential to determine the functional roles of key taxa, particularly C15 variants, C116, as well as C55 and other low-abundance *Cladocopium* lineages, and to assess how these symbiotic partnerships influence holobiont performance and long-term reef persistence in the eastern Indian Ocean under future climate scenarios.

**Acknowledgements** We respectfully acknowledge the Baiyungu, Thalanyji, Yinigurdira, Bindal, Noongar Wadjak and Wulgurukaba people, the Traditional Owners and custodians of the land and sea country upon which our research was conducted. We are grateful to the present and former Minderoo Exmouth Research Laboratory staff members and our dedicated volunteers for their involvement in field operations. We extend special thanks to the Conservation 'Omics lab, Mahsa Mousavi-Derazmahalleh, and Niko Andreakis for the lab and bioinformatic support.

**Author contributions** All authors contributed to the conception and design of the study. K.M.Q., D.J., and Z.T.R. obtained permits, permissions, and funding for the project. L.K. and D.J. conducted fieldwork and lab processing of samples. D.J. performed *Porites* morphological assessment and host species identification. L.K. performed DNA extraction, quantification, PCR amplification, and analysis of Symbiodiniaceae data. L.K. wrote the original draft of the manuscript and all authors reviewed and provided edits to the manuscript. All authors approved the final version of the manuscript for publication.

**Funding** Open Access funding enabled and organized by CAUL and its Member Institutions. This research was conducted under the Minderoo Foundation grants: GCA*Porites–346626.4 to Z.T.R. and D.J., Putting MERL on the Map to K.M.Q and was a collaborative effort between James Cook University, Minderoo Foundation, Curtin University, and the Department of Biodiversity, Conservation, and Attractions. K.M.Q. is supported by funding from ARC DECRA Fellowship (DE230100284) and Minderoo Foundation.*

**Data availability** Datasets and scripts that support the results of this study can be accessed through Github [https://github.com/lindseykraemer/Ningaloo_Porites]. Sequencing data are available on the NCBI Sequence Read Archive under the Bioproject accession number PRJNA1433380.

**Declarations**

**Conflict of interest** The authors declare no competing interest.

**Ethical approval** Samples were collected under DBCA Fauna Taking Licences #FO25000342-3 and #FO25000458 and the Department of Primary Industries and Regional Development, Western Australia exemptions #251145223 and #251143023.



## References

Ainsworth TD, Vega Thurber RL, Gates RD (2010) The future of coral reefs: a microbial perspective. Trends Ecol Evol 25:233–240

Anderson MJ, Ellingsen KE, McArdle BH (2006) Multivariate dispersion as a measure of beta diversity. Ecol Lett 9:683–693

Anderson MJ (2017) Permutational Multivariate Analysis of Variance (PERMANOVA). Wiley StatsRef: Statistics Reference Online 1–15

Arif C, Daniels C, Bayer T, Banguera-Hinestroza E, Barbrook A, Howe CJ, LaJeunesse TC, Voolstra CR (2014) Assessing *Symbiodinium* diversity in scleractinian corals via next-generation sequencing-based genotyping of the ITS2 rDNA region. Mol Ecol 23:4418–4433

Baker AC (2003) Flexibility and specificity in coral-algal symbiosis: diversity, ecology, and biogeography of *Symbiodinium*. Annu Rev Ecol Evol Syst 34:661–689

Baker AC, Starger CJ, McClanahan TR, Glynn PW (2004) Corals' adaptive response to climate change. Nature 430:741

Baker AC, Glynn PW, Riegl B (2008) Climate change and coral reef bleaching: an ecological assessment of long-term impacts, recovery trends and future outlook. Estuar Coast Shelf Sci 80:435–471

Berkelmans R, van Oppen MJH (2006) The role of zooxanthellae in the thermal tolerance of corals: a 'nugget of hope' for coral reefs in an era of climate change. Proc Biol Sci 273:2305–2312

Bernard H (1905) The family Poritidae. II. - The genus Porites. Part I. - Porites of the Indo-Pacific Region. In: Catalogue of the Madreporarian Corals in the British Museum (Natural History. pp 1–303

Budd AF, Johnson KG, Potts DC (1994) Recognizing morphospecies in colonial reef corals: I. landmark-based methods. Paleobiology 20:484–505

Buddemeier RW, Baker AC, Fautin DG, Jacobs JR (2004) The Adaptive Hypothesis of Bleaching. In: Rosenberg E, Loya Y (eds) Coral Health and Disease. Springer, Berlin, Heidelberg, Berlin, Heidelberg, pp 427–444

Callahan BJ, McMurdie PJ, Rosen MJ, Han AW, Johnson AJA, Holmes SP (2016) DADA2: high-resolution sample inference from Illumina amplicon data. Nat Methods 13:581–583

Camacho C, Coulouris G, Avagyan V, Ma N, Papadopoulos J, Bealer K, Madden TL (2009) BLAST+: architecture and applications. BMC Bioinformatics 10:421

Claar DC, Starko S, Tietjen KL, Epstein HE, Cunning R, Cobb KM, Baker AC, Gates RD, Baum JK (2020) Dynamic symbioses reveal pathways to coral survival through prolonged heatwaves. Nat Commun 11:6097

Correa AMS, Baker AC (2009) Understanding diversity in coral-algal symbiosis: A cluster-based approach to interpreting fine-scale genetic variation in the genus *Symbiodinium*. Coral Reefs 28:81–93

Cunning R, Gates RD, Edmunds PJ (2017) Using high-throughput sequencing of *Symbiodinium* metacommunities in St. John, US Virgin Islands. PeerJ 5:e3472

Davies SW, Gamache MH, Howe-Kerr LI, Kriefall NG, Baker AC, Banaszak AT, Bay LK, Bellantuono AJ, Bhattacharya D, Chan CX, Claar DC, Coffroth MA, Cunning R, Davy SK, del Campo J, Díaz-Almeyda EM, Frommlet JC, Fuess LE, González-Pech RA, Goulet TL, Hoadley KD, Howells EJ, Hume BCC, Kemp DW, Kenkel CD, Kitchen SA, LaJeunesse TC, Lin S, McIlroy SE, McMinds R, Nitschke MR, Oakley CA, Peixoto RS, Prada C, Putnam HM, Quigley K, Reich HG, Reimer JD, Rodriguez-Lanetty M, Rosales SM, Saad OS, Sampayo EM, Santos SR, Shoguchi E, Smith EG, Stat M, Stephens TG, Strader ME, Suggett DJ, Swain TD, Tran C, Traylor-Knowles N, Voolstra CR, Warner ME, Weis VM, Wright RM, Xiang T, Yamashita H, Ziegler M, Correa AMS, Parkinson JE (2023) Building consensus around the assessment and interpretation of Symbiodiniaceae diversity. PeerJ 11:e15023

Depczynski M, Gilmour JP, Ridgway T, Barnes H, Heyward AJ, Holmes TH, Moore JAY, Radford BT, Thomson DP, Tinkler P, Wilson SK (2013) Bleaching, coral mortality and subsequent survivorship on a West Australian fringing reef. Coral Reefs 32:233–238

Dunnington D, Thorne B, Hernangomez D (2023) ggspatial: Spatial Data Framework for ggplot2. CRAN

Fox J, Weisberg S (2019) An R Companion to Applied Regression.

Frøslev TG, Kjøller R, Bruun HH, Ejrnæs R, Brunbjerg AK, Pietroni C, Hansen AJ (2017) Algorithm for post-clustering curation of DNA amplicon data yields reliable biodiversity estimates. Nat Commun 8:1188

Gardner SG, Camp EF, Smith DJ, Kahlke T, Osman EO, Gendron G, Hume BCC, Pogoreutz C, Voolstra CR, Suggett DJ (2019) Coral microbiome diversity reflects mass coral bleaching susceptibility during the 2016 El Niño heat wave. Ecol Evol 9:938–956

Gleeson MW, Strong AE (1995) Applying MCSST to coral reef bleaching. Adv Space Res 16:151–154

Grupstra CGB, Meyer-Kaiser KS, Bennett M, Andres MO, Juszkiewicz DJ, Fifer JE, Da-Anoy JP, Gomez-Campo K, Martinez-Rugerio I, Aichelman HE, Huzar AK, Hughes AM, Rivera HE, Davies SW (2024) Holobiont Traits Shape Climate Change Responses in Cryptic Coral Lineages. Glob Chang Biol 30:

Heron SF, Maynard JA, van Hooidonk R, Eakin CM (2016) Warming Trends and Bleaching Stress of the World's Coral Reefs 1985–2012. Sci Rep 6:38402

Heron SF, Liu G, Eakin CM, Skirving WJ, Muller-Karger FE, Vega-Rodriguez M, De La Cour JL, Burgess TFR, Strong AE, Geiger EF, Guild LS, Lynds S (2014) Climatology development for NOAA Coral Reef Watch's 5-km product suite. NOAA technical report NESDIS 145:

Hoegh-Guldberg O (1999) Climate change, coral bleaching and the future of the world's coral reefs. Mar Freshw Res 50:839–866

Howells EJ, Beltran VH, Larsen NW, Bay LK, Willis BL, van Oppen MJH (2012) Coral thermal tolerance shaped by local adaptation of photosymbionts. Nat Clim Chang 2:116–120

Hughes TP, Kerry JT, Baird AH, Connolly SR, Dietzel A, Eakin CM, Heron SF, Hoey AS, Hoogenboom MO, Liu G, McWilliam MJ, Pears RJ, Pratchett MS, Skirving WJ, Stella JS, Torda G (2018) Global warming transforms coral reef assemblages. Nature 556:492–496

Hume BCC, Smith EG, Ziegler M, Warrington HJM, Burt JA, LaJeunesse TC, Wiedenmann J, Voolstra CR (2019) SymPortal: a novel analytical framework and platform for coral algal symbiont next-generation sequencing *ITS2* profiling. Mol Ecol Resour 19:1063–1080

Illumina Inc (2017) bcl2fastq2 Conversion Software v2.20. https://support.illumina.com/downloads/bcl2fastq-conversion-software-v2-20.html

Lahti L, Shetty S (2017) Tools for microbiome analysis in R. Version 1.24.0. http://microbiome.github.com/microbiome

LaJeunesse TC, Thornhill DJ, Cox EF, Stanton FG, Fitt WK, Schmidt GW (2004) High diversity and host specificity observed among symbiotic dinoflagellates in reef coral communities from Hawaii. Coral Reefs 23:596–603

LaJeunesse TC, Parkinson JE, Gabrielson PW, Jeong HJ, Reimer JD, Voolstra CR, Santos SR (2018) Systematic revision of Symbiodiniaceae highlights the antiquity and diversity of coral endosymbionts. Curr Biol 28:2570-2580.e6

Levas SJ, Grottoli AG, Hughes A, Osburn CL, Matsui Y (2013) Physiological and biogeochemical traits of bleaching and recovery in the mounding species of coral *Porites lobata*: implications for resilience in mounding corals. PLoS ONE 8:e63267

Lewis RE, Davy SK, Gardner SG, Rongo T, Suggett DJ, Nitschke MR (2022) Colony self-shading facilitates Symbiodiniaceae cohabitation in a South Pacific coral community. Coral Reefs 41:1433–1447

Love MI, Huber W, Anders S (2014) Moderated estimation of fold change and dispersion for RNA-seq data with DESeq2. Genome Biol 15:550

Lozupone CA, Hamady M, Kelley ST, Knight R (2007) Quantitative and qualitative β diversity measures lead to different insights into factors that structure microbial communities. Appl Environ Microbiol 73:1576–1585

McKnight DT, Huerlimann R, Bower DS, Schwarzkopf L, Alford RA, Zenger KR (2019) Methods for normalizing microbiome data: an ecological perspective. Methods Ecol Evol 10:389–400

McMurdie PJ, Holmes S (2013) Phyloseq: an R package for reproducible interactive analysis and graphics of microbiome census data. PLoS ONE 8:e61217

McMurdie PJ, Holmes S (2014) Waste not, want not: why rarefying microbiome data is inadmissible. PLoS Comput Biol 10:e1003531

Pichon Michel, Veron JEN (1982) Part IV Family Portidae: Australian Institute of Marine Science Monograph Series. In: Scleractinia of Eastern Australia. Australian National University Press, Canberra.,

Muscatine L (1990) The role of symbiotic algae in carbon and energy flux in reef corals. Ecosyst World 25:75–87

Muscatine L, D'Elia CF (1978) The uptake, retention, and release of ammonium by reef corals 1. Limnol Oceanogr 23:725–734

NOAA Coral Reef Watch (2024) NOAA Coral Reef Watch Version 3.5 Daily Global 5km Satellite Thermal History Product. https://www.star.nesdis.noaa.gov/pub/socd/mecb/crw/data/thermal_history/v3.5/

Oksanen J, Simpson GL, Blanchet FG, Kindt R, Legendre P, Minchin PR, O'Hara RB, Solymos P, Stevens MHH, Szoecs E, Wagner H, Barbour M, Bedward M, Bolker B, Borcard D, Carvalho G, Chirico M, De Caceres M, Durand S, Evangelista H, FitzJohn R, Friendly M, Furneaux B, Hannigan G, Hill M, Lahti L, McGlinn D, Ouellette M, Ribeiro Cunha E, Smith T, Stier A, Ter Braak C, Weedon J (2022) vegan: Community Ecology Package. R package version 2.6–4. https://CRAN.R-project.org/package=vegan

Paradis E, Claude J, Strimmer K (2004) APE: analyses of phylogenetics and evolution in R language. Bioinformatics 20:289–290

Pebesma E (2018) Simple features for R: standardized support for spatial vector data. R J 10:439–446

Pochon X, Pawlowski J, Zaninetti L, Rowan R (2001) High genetic diversity and relative specificity among *Symbiodinium*-like endosymbiotic dinoflagellates in soritid foraminiferans. Mar Biol 139:1069–1078

Pootakham W, Mhuantong W, Putchim L, Yoocha T, Sonthirod C, Kongkachana W, Sangsrakru D, Naktang C, Jomchai N, Thongtham N, Tangphatsornruang S (2018) Dynamics of coral-associated microbiomes during a thermal bleaching event. Microbiologyopen 7:e00604

Putnam HM, Stat M, Pochon X, Gates RD (2012) Endosymbiotic flexibility associates with environmental sensitivity in scleractinian corals. Proc R Soc B Biol Sci 279:4352–4361

Putnam HM, Barott KL, Ainsworth TD, Gates RD (2017) The vulnerability and resilience of reef-building corals. Curr Biol 27:R528–R540

Qin Z, Yu K, Chen B, Wang Y, Liang J, Luo W, Xu L, Huang X (2019) Diversity of Symbiodiniaceae in 15 Coral Species From the Southern South China Sea: Potential Relationship With Coral Thermal Adaptability. Front Microbiol 10:

Quigley KM, Davies SW, Kenkel CD, Willis BL, Matz MV, Bay LK (2014) Deep-sequencing method for quantifying background abundances of *Symbiodinium types*: Exploring the rare *Symbiodinium* biosphere in reef-building corals. PLoS ONE 9:e94297

Quigley KM, Willis BL, Kenkel CD (2019) Transgenerational inheritance of shuffled symbiont communities in the coral *Montipora digitata*. Sci Rep 9:13328

Quigley KM, Ramsby B, Laffy P, Harris J, Mocellin VJL, Bay LK (2022) Symbioses are restructured by repeated mass coral bleaching. Sci Adv 8:eabq8349

R Core Team (2021) R: A language and environment for statistical computing. https://www.R-project.org

Richards ZT, Haines L, Ross C, Preston S, Matthews T, Terriaca A, Black E, Lewis Y, Mannolini J, Dean P, Middleton V, Saunders B (2024) Deoxygenation following coral spawning and low-level thermal stress trigger mass coral mortality at Coral Bay, Ningaloo Reef. Coral Reefs 43:443–453

Silverstein RN, Cunning R, Baker AC (2015) Change in algal symbiont communities after bleaching, not prior heat exposure, increases heat tolerance of reef corals. Glob Change Biol 21:236–249

Skirving W, Marsh B, De La Cour J, Liu G, Harris A, Maturi E, Geiger E, Eakin CM (2020) CoralTemp and the Coral Reef Watch coral bleaching heat stress product suite version 3.1. Remote Sens 12:3856

Smith A, Cook N, Cook K, Brown R, Woodgett R, Veron J, Saylor V (2021) Field measurements of a massive *Porites* coral at Goolboodi (Orpheus Island), Great Barrier Reef. Sci Rep 11:15334

Starko S, Fifer JE, Claar DC, Davies SW, Cunning R, Baker AC, Baum JK (2023) Marine heatwaves threaten cryptic coral diversity and erode associations among coevolving partners. Sci Adv 9:eadf0954

Stat M, Pochon X, Cowie ROM, Gates RD (2009) Specificity in communities of *Symbiodinium* in corals from Johnston Atoll. Mar Ecol Prog Ser 386:83–96

Strong AE, Barrientos CS, Duda C, Sapper J (1997) Improved satellite techniques for monitoring coral reef bleaching. 1495–1498

Sully S, Burkepile DE, Donovan MK, Hodgson G, van Woesik R (2019) A global analysis of coral bleaching over the past two decades. Nat Commun 10:1264

Swain TD, Chandler J, Backman V, Marcelino L (2016) Consensus thermotolerance ranking for 110 *Symbiodinium* phylotypes: an exemplar utilization of a novel iterative partial-rank aggregation tool with broad application potential. Funct Ecol 31:172–183

Tan YTR, Wainwright BJ, Afiq-Rosli L, Ip YCA, Lee JN, Nguyen NTH, Pointing SB, Huang D (2020) Endosymbiont diversity and community structure in *Porites lutea* from Southeast Asia are driven by a suite of environmental variables. Symbiosis 80:269–277

Terraneo TI, Houlbreque F, Arrigoni R, Longari B, Berumen ML, Hume BCC, Fiat S, Rodolfo-Metalpa R, Payri CE, Voolstra CR, Benzoni F (2024) Coral-associated Symbiodiniaceae dynamics during the 2016 mass bleaching event in New Caledonia. Coral Reefs 43:1127–1132

Tonk L, Sampayo EM, LaJeunesse TC, Schrameyer V, Hoegh-Guldberg O (2014) *Symbiodinium* (Dinophyceae) diversity in reef-invertebrates along an offshore to inshore reef gradient near Lizard Island, Great Barrier Reef. J Phycol 50:552–563

UNESCO (2023) Boundaries of UNESCO World Heritage Marine Sites (v02). https://www.marineregions.org/

Vanderklift MA, Babcock RC, Barnes PB, Cresswell AK, Feng M, Haywood MDE, Holmes TH, Lavery PS, Pillans RD, Smallwood CB, Thomson DP, Tucker AD, Waples K, Wilson SK (2020) The oceanography and marine ecology of Ningaloo, a World Heritage Area. In: Oceanography and Marine Biology : An Annual Review. CRC Press, pp 143–178

Vaughan TW (1907) Recent Madreporaria of the Hawaiian Islands and Laysan. U S Natl Mus Bull 9:1–427

Vaughan TW (1918) Some shallow-water corals from Murray Island (Australia), Cocos-Keeling Island, and Fanning Island. Pap Dep Mar Biol Carnegie Inst Wash 9:49–234

Veron JEN (1985) New Scleractinia from Australian coral reefs. Rec West Aust Mus 12:147–183

Veron JEN (1986) Corals of Australia and the Indo-Pacific. Angus & Robertson, North Ryde, N.S.W

Veron JEN (1993) A biogeographic database of hermatypic coral species of the central Indo-Pacific, genera of the world. Australian Institute of Marine Science, Townsville, Qld, Townsville, Qld

Veron JEN, Marsh LM (1988) Hermatypic corals of Western Australia : records and annotated species list. Western Australian Museum, Perth, WA, Perth, WA

Voolstra CR, Suggett DJ, Peixoto RS, Parkinson JE, Quigley KM, Silveira CB, Sweet M, Muller EM, Barshis DJ, Bourne DG, Aranda M (2021) Extending the natural adaptive capacity of coral holobionts. Nat Rev Earth Environ 2:747–762

Wang Q, Garrity GM, Tiedje JM, Cole JR (2007) Naïve Bayesian classifier for rapid assignment of rRNA sequences into the new bacterial taxonomy. Appl Environ Microbiol 73:5261–5267

Wernberg T, Thomsen MS, Baum JK, Bishop MJ, Bruno JF, Coleman MA, Filbee-Dexter K, Gagnon K, He Q, Murdiyarso D, Rogers K, Silliman BR, Smale DA, Starko S, Vanderklift MA (2024) Impacts of climate change on marine foundation species. Annu Rev Mar Sci 16:247–282

Wickham H (2016) ggplot2: Elegant Graphics for Data Analysis. Springer International Publishing, Cham

Zhu A, Ibrahim JG, Love MI (2019) Heavy-tailed prior distributions for sequence count data: removing the noise and preserving large differences. Bioinformatics 35:2084–2092

Ziegler M, Roder C, Büchel C, Voolstra CR (2015) Niche acclimatization in Red Sea corals is dependent on flexibility of host-symbiont association. Mar Ecol Prog Ser 533:149–161

Ziegler M, Eguíluz VM, Duarte CM, Voolstra CR (2018) Rare symbionts may contribute to the resilience of coral–algal assemblages. ISME J 12:161–172